

1 **Active geothermal systems with entrained seawater as analogues for low-sulphidation**
2 **epithermal mineralization**

3 Jonathan Naden,
4 British Geological Survey, Keyworth, Nottingham, NG12 5GG, UK

5 Stephanos P. Kiliadis
6 Department of Economic Geology and Geochemistry, University of Athens,
7 Panepistimioupolis, Zographou, 157 84, Athens, Greece

8 D.P. Fiona Darbyshire
9 NERC Isotope Geosciences Laboratory, British Geological Survey, Keyworth Nottingham,
10 NG12 5GG, UK.

11 **Abstract (207 words)**

12 The paradigm for low-sulphidation (LS) volcanic-arc associated mineralization is the active
13 geothermal systems located along the Taupo Volcanic Zone (e.g. Broadlands). However, this
14 analogue is inapt where fluid salinities are consistently in excess of 3.5 wt % NaCl.

15 LS mineralization on Milos (Aegean arc) records high paleofluid-salinities. The δD and $\delta^{18}O$
16 data do not exemplify ^{18}O -shifted meteoric waters—typical of terrestrial geothermal systems.
17 Nor is a submarine origin indicated—stable isotope data show mixing between meteoric,
18 seawater and volcanic-arc gases. Strontium isotope data are comparable to a nearby active
19 seawater-entrained geothermal system. These are features seen in hydrothermal systems
20 associated with emergent volcanoes.

21 For the Milos LS mineralization, high-salinity fluids show it cannot be explained by a
22 Broadlands-type model. The absence of saliferous sequences and significant intrusive rocks
23 preclude these as salinity sources. The similarities between paleo and active systems in terms
24 of salinity, δD – $\delta^{18}O$ and strontium isotope systematics strongly suggest that seawater is the
25 main source for Na and Cl. We suggest geothermal systems, containing seawater, associated
26 with emergent volcanoes are an alternative analogue for LS epithermal mineralization.
27 Furthermore, they bridge the gap between submarine, and large-scale terrestrial geothermal
28 systems—the modern analogues for VHMS and epithermal mineralisation in the scheme of
29 intrusion-centered hydrothermal mineralization.

30 **Keywords**

31 Epithermal processes, seawater, Milos, isotopes

32 **Introduction**

33 Geothermal systems in convergent plate margin settings are the active equivalents of high-
34 level (2–3 km) intrusion-centred hydrothermal ore-deposits (e.g. Hedenquist and Lowenstern,
35 1994). Close to magmatic activity, volcanic emanations are the surface expressions of
36 porphyry-Cu and high-sulphidation epithermal-Au mineralizing processes at depth
37 (Hedenquist et al., 1993). Located farther from the magmatic source are low-sulphidation
38 (LS) epithermal deposits, for which the Broadlands–Ohaaki geothermal system is the
39 paradigm (e.g. Simmons and Browne, 2000). Generally, in LS mineralization, fluid inclusions
40 document low-salinity fluids (< 1 wt % dissolved salts + CO₂) and these are equivalent to the
41 low-chlorinity (< 1000 ppm) fluids seen in Broadlands-type geothermal systems. However,
42 they also identify saline fluids (up to 15 wt % salts) and, in this case, there are no documented
43 active analogues (Hedenquist and Lowenstern, 1994). Conversely, deep water (> 1000 m)
44 geothermal systems, such as TAG (e.g. You and Bickle, 1998) are exemplars for VHMS
45 deposits. However, where boiling submarine geothermal fluids vent into shallow water (< 200
46 m) mineralization is epithermal in style (Stoffers et al., 1999), but there are no clearly defined
47 ancient equivalents (Huston, 2000). Thus, in both the submarine and subaerial environments
48 there is a missing link between active geothermal systems and their ancient counterparts.

49 Below, we provide new strontium isotope data and summarize features of epithermal systems
50 on Milos island. By comparing these with well-characterised modern analogues we suggest
51 that active geothermal systems with entrained seawater, such as those in the Aegean arc
52 (Aegean arc-type), are an alternative to the Broadlands–Ohaaki LS paradigm in the scheme of
53 intrusion-centred hydrothermal systems.

54 **The Aegean arc**

55 The Aegean arc is a zone of Pliocene to modern volcanism related to active back-arc
56 extension caused by the subduction of the African plate beneath the Aegean micro-plate (e.g.
57 Pe-Piper and Piper, 2002). It is built on continental crust, comprises seven major volcanic
58 centres and is located 120–250 km north of the Hellenic trench (Fig. 1). The volcanic rocks
59 are calc-alkaline with localised high-K variants and range from basalt to rhyolite in
60 composition, with dominant andesites and dacites. Present day hydrothermal activity
61 comprises both low-enthalpy (Aegina, Sousaki, Methana) and high-enthalpy systems (Milos,
62 Nisyros).

63 *Milos geology and LS epithermal Au-Ag mineralization*

64 Upper Pliocene (2.66 ± 0.07 Ma; Stewart and McPhie, 2003) submarine and Late Pleistocene
65 to present (1.9–0.1 Ma) subaerial volcanic rocks overlay Mesozoic metamorphic basement
66 and Upper Miocene–Lower Pliocene marine sediments, and record a transition from a shallow
67 submarine (< 200 m) to subaerial volcanic setting (Fytikas et al., 1986; Rinaldi and Venuti,
68 2003; Stewart and McPhie, 2003). Emergence probably occurred at 1.44 ± 0.08 Ma (Stewart
69 and McPhie, 2003). Plutonic rocks are not known on Milos and have only been reported as
70 ignimbrite-hosted granitic xenoliths from the nearby islet of Kimolos (Pe-Piper and Piper,
71 2002).

72 The oldest submarine volcanic rocks occur on western Milos and host LS Au–Ag
73 mineralization (the Profitis Ilias [PI]–Chondro Vouno [CV] epithermal system), which
74 extends over a 20 km² area (this study; Kiliyas et al., 2001). Fluid inclusion data show the
75 hydrothermal fluids underwent extreme boiling and vaporisation. Importantly, final ice-
76 melting (T_{mice}) data show that 70 % of the fluid inclusions have net salinities in excess of
77 seawater (Tab. 1), showing that throughout its lifespan, fluids in the system were saline. The
78 tops of the paleosystem (now ~600 masl) show crustiform/colloform quartz–barite±alunite
79 veins and quartz-cemented breccias, with locally high gold (PI: 56 ppm; CV: 250 ppm) and
80 silver (PI: 197 ppm; CV: 90 ppm). Deeper in the system (now ~300 masl), the mineralization
81 is dominated by a base-metal-bearing stockwork. Elevated gold values at PI are concentrated
82 above the base metal zone and are spatially related to boiling (Kiliyas et al., 2001).

83 *Active geothermal system*

84 In the active geothermal system (Liakopoulos, 1987; Pflumio et al., 1991), data indicate a
85 two-component reservoir: (1) A high enthalpy system with deep seawater recharge located 1–
86 2 km below sea-level. Reservoir temperatures range 250–350 °C and salinities can be
87 significantly higher than seawater (up to 9 wt % salts). This results from Rayleigh distillation
88 as seawater percolates, through progressively hotter rocks, into the reservoir. Due to its high
89 salinity, venting of the deep geothermal fluid is accompanied by boiling close to the top of the
90 reservoir and in some cases the reservoir may be two-phase. (2) A shallow reservoir (100–175
91 °C) overlies the high-enthalpy system. It is located close to sea-level, recharged by meteoric
92 water and seawater intrusion, is commonly saline (up to 5 wt % salts) and heated by gas
93 escapes from the underlying deep reservoir. Seawater, as a major component of both the deep

94 and shallow reservoirs, is documented on the basis of $^{87}\text{Sr}/^{86}\text{Sr}$ and $\delta\text{D}-\delta^{18}\text{O}-\text{Cl}$ systematics
95 (Pflumio et al., 1991). In the shallow (<100 m) submarine environment, venting geothermal
96 fluids contain suspended particulate matter strongly enriched in Fe, Mn, Si and Ba and locally
97 deposit APS minerals, pyrite, marcasite, barite, gypsum, and calcite (Baltatzis et al., 2001;
98 Varnavas et al., 2000). In addition, the deep reservoir is metalliferous (Pb: 180 ppb; Zn: 1458
99 ppb) (Christanis and Seymour, 1995) and has gold concentrations in the region of 0.3 ppb
100 (Liakopoulos, 1987).

101 *Strontium isotopes*

102 Sr-isotope data show that the least altered igneous rocks have low $^{87}\text{Sr}/^{86}\text{Sr}$, whereas their
103 hydrothermally altered counterparts are closer to a seawater signature (Fig. 2). The basement
104 rocks have variable strontium ratios (0.7033–0.7136) (Fig. 2). In the modern system,
105 $^{87}\text{Sr}/^{86}\text{Sr}$ in the fluids vary from 0.7092–0.7102 (Pflumio et al., 1991). Barites from the
106 Profitis Ilias mineralization display similar $^{87}\text{Sr}/^{86}\text{Sr}$ to the modern system (Fig. 2). All values
107 for geothermal water and hydrothermal minerals are slightly more radiogenic than seawater
108 but relatively constant.

109 **Discussion**

110 *Seawater as a fluid component on Milos*

111 T_{mice} in fluid inclusions provides information on salinity. However, above $-1.5\text{ }^{\circ}\text{C}$, it is unable
112 to distinguish between dissolved salt (< 2.5 wt % NaCl eq.) and gas (< 4.4 wt % CO_2 eq.).
113 This permits gas-charged low-chlorinity terrestrial geothermal systems to be the paradigm for
114 LS epithermal mineralization, as excess chlorinity can be assigned to dissolved gas
115 (Hedenquist and Henley, 1985). Moreover, in Broadlands–Ohaaki-type geothermal systems
116 derivation of chlorinities in excess of 5000 ppm through fluid–rock interaction is extremely
117 difficult and where high salinities are recorded they are attributed to boiling to dryness and
118 have a localised effect (Simmons and Browne, 1997). Hence, when comparing ancient
119 systems with Broadlands–Ohaaki-type equivalents, when the apparent salinity is up to 3–4 wt
120 % NaCl eq there is an implicit requirement to assign freezing point depressions to dissolved
121 gas rather than chlorinity. However, in our case > 70 % of the fluid inclusions have net
122 salinities in excess of 3.5 wt % NaCl eq (Tab. 1). Thus, we cannot assign excess T_{mice} to
123 dissolved gas. Nonetheless, our high salinities have to be explained. There are three main
124 sodium and chlorine reservoirs available to large-scale geothermal systems: (1) evaporites and

125 evaporitic sediments (2) magmatic brines and (3) seawater. An evaporitic origin of salinity is
126 considered highly improbable, as there is no record of saliferous rocks within the Milos
127 sediments. Concerning a magmatic brine, it is estimated that during its lifetime a geothermal
128 systems turns over between $10^{6\pm 1}$ km³ of water (Barnes and Seward, 1997). If it is assumed
129 that andesitic magmas contain about 1000 ppm chlorine, then approximately $10^{7\pm 1}$ km³ of
130 magma would be required maintain salinities in the geothermal system at 9 wt % NaCl. This
131 is not impossible, but on Milos, geological and geophysical evidence is lacking (Pe-Piper and
132 Piper 2002). Thus, a magmatic origin of salinity is also considered unlikely. This leaves a
133 seawater origin for Na and Cl. We consider that the chemical similarities between the ancient
134 and modern systems on Milos (see above) support a seawater origin for the PI–CV epithermal
135 fluids.

136 Comparison of δD – $\delta^{18}O$ of inclusion fluids from the Profitis Ilias epithermal mineralization
137 and several active geothermal systems associated with emergent volcanoes reveals remarkable
138 similarities (Fig. 3). In the active systems, the geothermal fluids have a three component
139 source (sea, meteoric and magmatic) and the waters fall in a zone projecting from the
140 meteoric water line to values intermediate to seawater and volcanic-arc gases (Fig. 3). The
141 fluid inclusion data for the Profitis Ilias LS mineralization show an analogous trend and lie in
142 a similar zone; this is in sharp contrast to typical LS mineralization where stable isotope data
143 show ¹⁸O-shifted fluids at constant δD (see Broadlands field in Fig. 3).

144 In terms of strontium isotope data (Fig. 2, the basement metamorphic sequence has ⁸⁷Sr/⁸⁶Sr
145 (0.7033–0.7137) encompassing the entire range, permitting a variety of fluid–rock interaction
146 interpretations. However, we think the clustering of measured ⁸⁷Sr/⁸⁶Sr for the modern
147 geothermal fluids (0.7092–0.7100) and mineralization (0.7096–0.7100 [epithermal Au–Ag];
148 0.7092–0.7098 [Mn–Ba] close to the value for late-Pliocene seawater (0.7090–0.7096), also
149 indicates of a seawater source. In addition, as ⁸⁷Sr/⁸⁶Sr for the modern and ancient systems are
150 significantly different from most of the unaltered igneous rocks (0.7050–0.7080) mitigates
151 further against a magmatic fluid source. Indeed, most of the ⁸⁷Sr/⁸⁶Sr (0.7082–0.7098) for
152 hydrothermally altered igneous rocks cluster within or close to the range recorded by the
153 modern geothermal fluids and seawater.

154 Taken together, the above lines of evidence show that in addition to being a fundamental
155 component in the active system, seawater has played a key role in LS mineralization.

156 *Hybrid epithermal systems and modern analogues*

157 It is clear that Broadlands–Ohaaki-type meteoric geothermal systems are not a valid analogue
158 for the Milos Au–Ag mineralization and for moderately saline (> 15 000 ppm NaCl eq.) LS
159 epithermal mineralization in general. Furthermore, there is a missing link between saline
160 epithermal LS systems and their modern counterparts. We suggest that the best candidates,
161 which recognize the key parameters of consistently high fluid inclusion salinities, δD – $\delta^{18}O$
162 systematics indicating seawater and a seawater Sr isotope signature, are geothermal systems
163 with entrained seawater. Typical examples are the active systems on Milos and Nisyros (Fig.
164 3). These analogues are hybrids, containing elements of both submarine and terrestrial
165 geothermal systems. Indeed, the occurrence of fossil hybrid systems is predicted (Huston,
166 2000) though, to date, no ancient equivalents have been clearly identified. Here, in the
167 emergent environment, circulating sea and meteoric water are the main fluid components. The
168 fluids boil and result in auriferous quartz veins with epithermal textures and proximal quartz-
169 adularia, intermediate quartz–sericite–pyrite and distal propylitic/quartz–albite alteration
170 halos—features that are comparable to the Milos epithermal mineralization. Thus, we suggest
171 that epithermal mineralization where the involvement of seawater can be clearly demonstrated
172 (e.g. Milos) are good candidates for fossil hybrid epithermal systems, and active geothermal
173 systems with entrained seawater such as the Aegean-arc type, are their modern analogues.

174 Features of hybrid epithermal systems can be reconstructed by putting geothermal systems
175 associated with emergent volcanoes into a conceptual framework. Fig. 4 illustrates the
176 model—gold-bearing epithermal veins are located between a shallow low-temperature (100–
177 175 °C) steam-heated zone recharged by meteoric water and seawater intrusion, and a deep,
178 seawater recharged, higher-temperature (250–350 °C) base-metal bearing reservoir.

179 **Concluding remarks**

180 Broadlands-type models are not appropriate for LS epithermal systems with elevated salinities
181 that cannot be reasonably explained by dissolved gas or localised boiling to dryness.
182 Moreover, where high salinities of this nature are encountered, an explanation for them must
183 be sought. One possibility is a seawater origin for the hydrothermal fluids, though to use this
184 explanation, other parameters have to be consistent. In the case of Milos, the epithermal
185 mineralization can be explained by analogy to seawater-entrained geothermal systems
186 associated with emergent volcanoes (e.g. Nisyros, Milos) and the mineralization data

187 (geologic, isotope and fluid inclusion) are in accord with this model. We suggest that our
188 Aegean-arc model should be considered as an additional paradigm in the scheme of intrusion-
189 centred metallogenesis. Moreover, it may provide a link between submarine and terrestrial
190 mineralization processes. Appropriate indicators for its use are fluid inclusion data showing
191 consistently elevated salinities (> 3.5 wt % NaCl eq.) and mineralization hosted in submarine
192 or transitional to subaerial volcanic rocks in an island arc tectonic setting. However, it must
193 be stressed that these are not definitive and other corroborating data must be sought, in our
194 case, strontium isotope, δD and $\delta^{18}O$ analyses.

195 **Acknowledgements**

196 This work was in part funded by a Marie Curie Experienced Researcher Fellowship to JN
197 (HPMF-CT-2000-00762) and University of Athens Research Committee Grants to SPK (KA
198 70/4/3373 and KA 70/4/6425). Royal Gold Inc. kindly provided access to proprietary data and
199 drill core. Melanie J Leng (NIGL) is thanked for undertaking some of the Sr-isotope analyses
200 JN publishes with permission of the Director, British Geological Survey, NERC. NERC
201 Isotope Geosciences Laboratory Publication No. xxxx

202 **References cited**

- 203 Baltatzis, E., Valsami-Jones, E., Magganas, A., and Kati, M., 2001, Tamarugite from Milos
204 island, Greece: *Neues Jahrbuch Fur Mineralogie-Monatshefte*, p. 371-377.
- 205 Barnes, H.L., and Seward, T.M., 1997, Geothermal systems and mercury deposits, *in* Barnes
206 Hubert, L., ed., *Geochemistry of Hydrothermal Ore Deposits*: New York, USA, John
207 Wiley & Sons, p. 699-736.
- 208 Briquieu, L., Javoy, M., Lancelot, J.R., and Tatsumoto, M., 1986, Isotope geochemistry of
209 recent magmatism in the Aegean arc: Sr, Nd, Hf, and O isotopic ratios in the lavas of
210 Milos and Santorini - geodynamic implications: *Earth and Planetary Science Letters*,
211 v. 80, p. 41-54.
- 212 Brombach, T., Caliro, S., Chiodini, G., Fiebig, J., Hunziker, J.C., and Raco, B., 2003,
213 Geochemical evidence for mixing of magmatic fluids with seawater, Nisyros
214 hydrothermal system, Greece: *Bulletin of Volcanology*, v. 65, p. 505-516.
- 215 Christanis, K., and Seymour, K.S., 1995, A study of scale deposition - an analog of
216 mesothermal to epithermal ore formation in the volcano of Milos, Aegean-arc, Greece:
217 *Geothermics*, v. 24, p. 541-552.
- 218 Farrell, J.W., Clemens, S.C., and Gromet, L.P., 1995, Improved chronostratigraphic reference
219 curve of late Neogene seawater Sr87/Sr86: *Geology*, v. 23, p. 403-406.

- 220 Field, C.W., and Fifarek, R.H., 1985, Light stable-isotope systematics in the epithermal
221 environment, *in* Berger, B.R., and Bethke, P.M., eds., *Geology and Geochemistry of*
222 *Epithermal Systems, Volume 2: Reviews in Economic Geology*, p. 99-128.
- 223 Fytikas, M., Innocenti, F., Kolios, N., Mannetti, P., Mazzuoli, R., Poli, G., Rita, F., and
224 Villari, L., 1986, Volcanology and petrology of volcanic products from the island of
225 Milos and neighbouring islets: *Journal of Volcanology and Geothermal Research*, v.
226 28, p. 297-317.
- 227 Giggenbach, W.F., 1992, Isotopic shifts in waters from geothermal and volcanic systems
228 along convergent plate boundaries and their origin: *Earth and Planetary Science*
229 *Letters*, v. 113, p. 495-510.
- 230 Hedenquist, J.W., and Henley, R.W., 1985, The importance of CO₂ on freezing-point
231 measurements of fluid inclusions - evidence from active geothermal systems and
232 implications for epithermal ore deposition: *Economic Geology*, v. 80, p. 1379-1406.
- 233 Hedenquist, J.W., and Lowenstern, J.B., 1994, The role of magmas in the formation of
234 hydrothermal ore deposits: *Nature*, v. 370, p. 519-527.
- 235 Hedenquist, J.W., Simmons, S.F., Giggenbach, W.F., and Eldridge, C.S., 1993, White Island,
236 New Zealand, volcanic-hydrothermal system represents the geochemical environment
237 of high-sulfidation Cu and Au ore deposition: *Geology*, v. 21, p. 731-734.
- 238 Hein, J.R., Stamatakis, M.G., and Dowling, J.S., 2000, Trace metal-rich Quaternary
239 hydrothermal manganese oxide and barite deposit, Milos Island, Greece: *Transactions*
240 *of the Institution of Mining and Metallurgy Section B-Applied Earth Science*, v. 109,
241 p. B67-B76.
- 242 Huston, D.L., 2000, Gold in volcanic-hosted massive sulfide deposits; distribution, genesis,
243 and exploration, *in* S.G., H., and P.E., B., eds., *Gold in 2000.*, Volume 13: *Reviews in*
244 *Economic Geology*, p. 401-426.
- 245 Kavouridis, T., Kuris, D., Leonis, C., Liberopoulou, V., Leontiadis, J., Panichi, C., La Ruffa,
246 G., and Caprai, A., 1999, Isotope and chemical studies for a geothermal assessment of
247 the island of Nisyros (Greece): *Geothermics*, v. 28, p. 219-239.
- 248 Kiliyas, S.P., Naden, J., Cheliotis, I., Shepherd, T.J., Constandinidou, H., Crossing, J., and
249 Simos, I., 2001, Epithermal gold mineralisation in the active Aegean Volcanic Arc:
250 the Profitis Ilias deposit, Milos Island, Greece: *Mineralium Deposita*, v. 36, p. 32-44.
- 251 Liakopoulos, A., 1987, *Hydrothermalisme et Mineralisations Metalliferes de l'ile de Milos*
252 *(Cyclades-Grece) [PhD thesis]*, Paris.
- 253 Naden, J., Kiliyas, S.P., Leng, M.J., and Cheliotis, I., 2003, Do fluid inclusions preserve δ¹⁸O
254 values of hydrothermal fluids in epithermal systems over geological time? Evidence
255 from paleo- and modern geothermal systems, Milos island, Aegean Sea: *Chemical*
256 *Geology*, v. 197, p. 143-159.
- 257 Pe-Piper, G., and Piper, D.J.W., 2002, *The Igneous Rocks of Greece*: Berlin, Germany,
258 Gebruder Borntraeger, 573 p.

- 259 Pflumio, C., Boulegue, J., Liakopoulos, A., and Briquieu, L., 1991, Oxygen, hydrogen,
260 strontium isotopes and metals in the present-day and past geothermal systems of Milos
261 Island (Aegean Arc), in Pagel, M., and J.L., L., eds., Source, Transport and Deposition
262 of Metals.: Rotterdam, Netherlands, A. A. Balkema, p. 107-112.
- 263 Rinaldi, M., and Venuti, M.C., 2003, The submarine eruption of the Bombarda volcano,
264 Milos Island, Cyclades, Greece: Bulletin of Volcanology, v. 65, p. 282-293.
- 265 Simmons, S.F., and Browne, P.R.L., 1997, Saline fluid inclusions in sphalerite from the
266 Broadlands- Ohaaki geothermal system: A coincidental trapping of fluids being boiled
267 toward dryness: Economic Geology, v. 92, p. 485-489.
- 268 —, 2000, Hydrothermal minerals and precious metals in the Broadlands-Ohaaki geothermal
269 system: Implications for understanding low-sulfidation epithermal environments:
270 Economic Geology, v. 95, p. 99-112.
- 271 Stewart, A.L., and McPhie, J., 2003, Facies architecture of the submarine- to subaerial
272 volcanic succession on Milos, Greece, The South Aegean Active Volcanic Arc:
273 Present Knowledge and Future Perspectives, Milos Conferences: Milos, Greece, p. 24.
- 274 Stoffers, P., Hannington, M., Wright, I., Herzig, P., and de Ronde, C., 1999, Elemental
275 mercury at submarine hydrothermal vents in the bay of plenty, Taupo volcanic zone,
276 New Zealand: Geology, v. 27, p. 931-934.
- 277 Varnavas, S.P., Panagiotaras, D., Megalovasilis, P., Dando, P., Alliani, S., and Meloni, R.,
278 2000, Compositional characterization of suspended particulate matter in Hellenic
279 Volcanic Arc Hydrothermal Centres: Physics and Chemistry of the Earth, Part B:
280 Hydrology, Oceans and Atmosphere, v. 25, p. 9-18.
- 281 You, C.F., and Bickle, M.J., 1998, Evolution of an active sea-floor massive sulphide deposit:
282 Nature, v. 394, p. 668-671.
- 283
284

284 Fig. 1. Maps showing **A)** the main geotectonic elements of the eastern Mediterranean along
285 with volcanic centres and regions of geothermal activity; **B)** the main geological features of
286 Milos island plus the location of LS epithermal mineralisation and the main surface
287 manifestations of the geothermal system (Milos map adapted from Fytikas et al., 1986; LPL:
288 Lower Pleistocene, LPo: Lower Pliocene; LMi: Lower Miocene, M: Mesozoic)

289 Fig. 2. 'S'-curve of measured strontium isotope data from mineralisation on Milos, showing
290 $^{87}\text{Sr}/^{86}\text{Sr}$ for barite, fresh and altered igneous rocks, marine platform sediments basement
291 rocks and geothermal waters (data: this study; Briquieu et al., 1986; Farrell et al., 1995; Hein
292 et al., 2000; Pflumio et al., 1991)

293 Fig. 3. Fluid-inclusion $\delta\text{D}-\delta^{18}\text{O}$ data for Profitis Ilias, comparing the epithermal
294 mineralisation with active systems on the Aegean arc with reference points for eastern
295 Mediterranean seawater (crossed squares labelled S) and estimated present day geothermal
296 liquids (filled triangles labelled M [Milos] and N [Nisyros]). (Milos epithermal mineralisation
297 data: Naden et al., 2003; geothermal data: Brombach et al., 2003; Kavouridis et al., 1999;
298 Liakopoulos, 1987; fields for volcanic arc gases and Broadlands derived from Giggenbach,
299 1992 and Field and Fifarek, 1985 respectively)

300 Fig. 4. Conceptual model of hybrid Aegean-arc-type epithermal systems (adapted from
301 Kavouridis et al., 1999; Liakopoulos, 1987)

302

302

303

304

305

306

307

308

309

310

311

312

TABLE 1. SUMMARY SALINITY DATA FOR PI-CV
EPITHERMAL AU-AG MINERALISATION

Deposit	Salinity (wt % NaCl eq.)					% FI with Tmice < -2.5 °C
	n	Min.	Max.	Mean	σ	
*CV	132	0.5	14.7	6.1	3.0	86%
†PI	139	0.0	11.3	5.2	2.1	71%

313

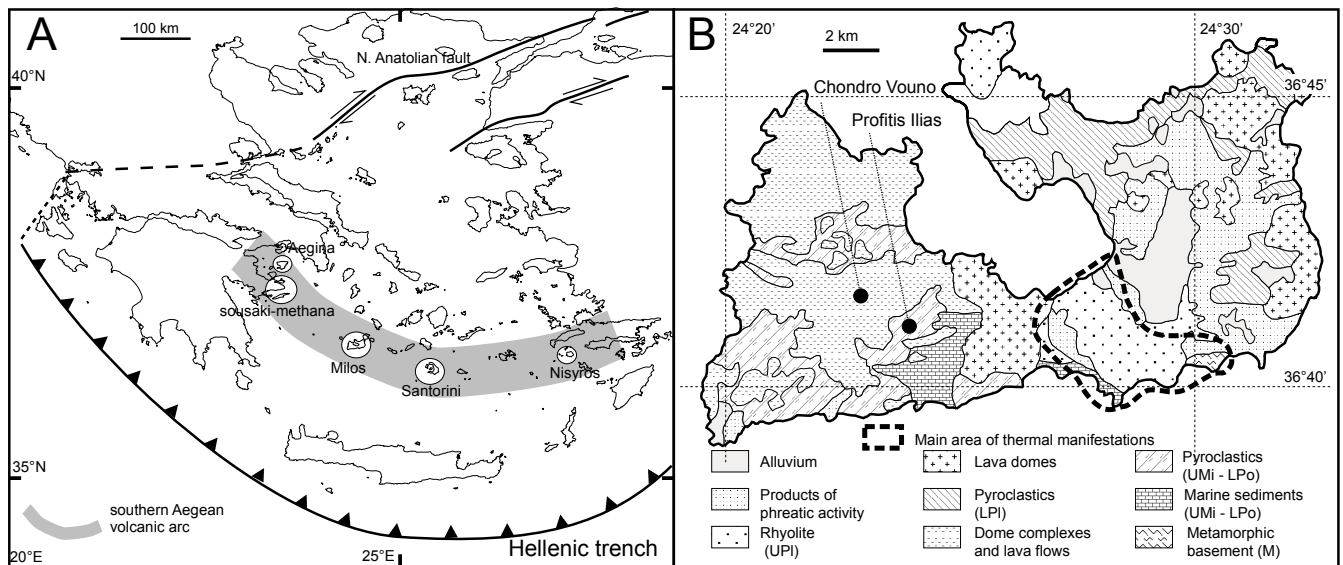
314

315

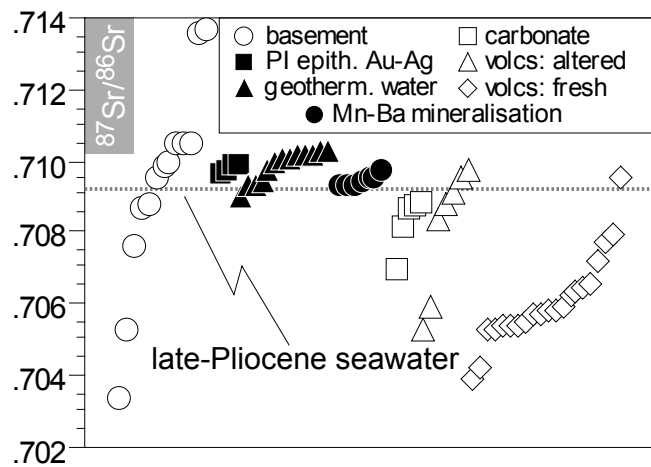
316

317

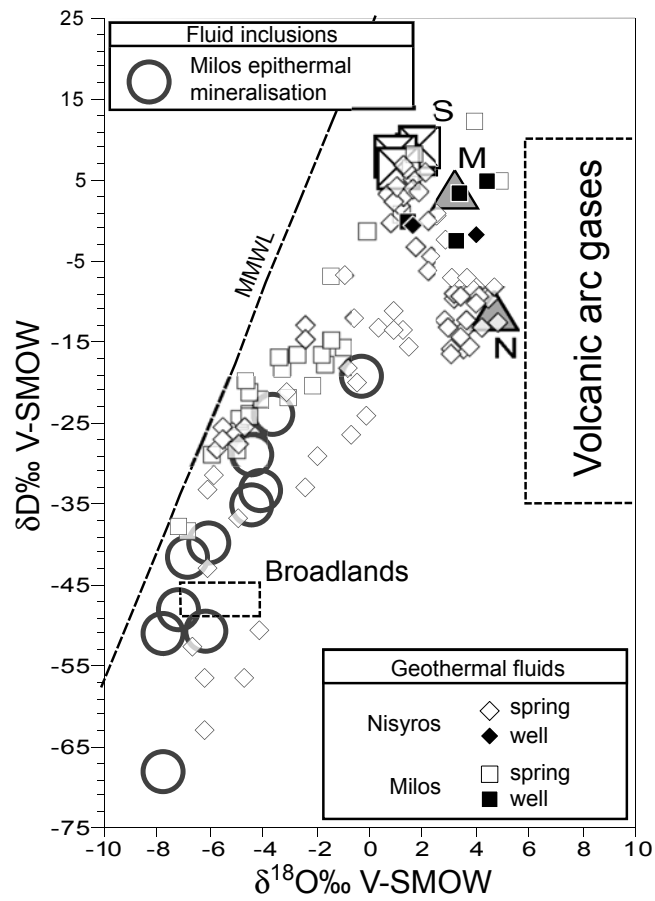
*this study
†Kiliyas et al., 2001



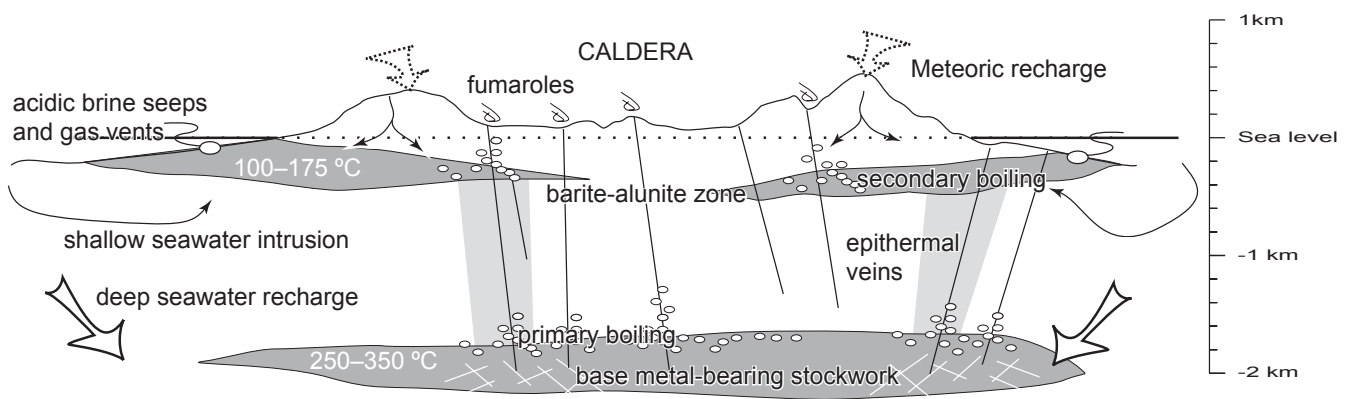
Naden et al: Geology, Fig. 1, actual size



Naden et al: Geology, Fig. 2, actual size



Naden et al: Geology, Fig. 3, Actual size



Naden et al: Geology, Fig. 4, actual size